# Influence of annealing on spin-dependent tunneling characteristics of fully epitaxial $Co_2MnGe/MgO/Co_{50}Fe_{50}$ magnetic tunnel junctions

Tomoyuki Taira, Takayuki Ishikawa, Naoki Itabashi, Ken-ichi Matsuda, Tetsuya Uemura, and Masafumi Yamamoto[a)]
*Division of Electronics for Informatics, Hokkaido University, Sapporo 060-0814, Japan*

(Received 16 December 2008; accepted 28 January 2009; published online 20 February 2009)

We found that the tunnel magnetoresistance ratio of fully epitaxial $Co_2MnGe/MgO/Co_{50}Fe_{50}$ magnetic tunnel junctions (MTJs) increased discontinuously and significantly from 92% at room temperature (RT) (244% at 4.2 K) for $T_a$ of 475 °C to 160% at RT (376% at 4.2 K) for $T_a$ of 500 °C, where $T_a$ is the temperature at which the MTJ trilayer was *in situ* annealed right after deposition of the upper electrode. We also found that the $dI/dV$ versus $V$ characteristics for the parallel and antiparallel magnetization configurations changed discontinuously and markedly with increasing $T_a$ from 475 °C or less to 500 °C or higher. These significant changes are discussed in terms of a possible change in the spin-dependent interfacial density of states. © *2009 American Institute of Physics*. [DOI: 10.1063/1.3083559]

Co-based Heusler alloys ($Co_2YZ$) attracted much interest as promising ferromagnetic electrode materials for spintronic devices, including magnetic tunnel junctions (MTJs),[1–6] giant magnetoresistance devices,[7,8] and for spin injection from ferromagnetic electrodes into semiconductors.[9,10] This is because of the half-metallic ferromagnetic nature theoretically predicted for many of these alloys[11–13] and because of their high Curie temperatures, which are well above room temperature (RT).[14] We recently developed fully epitaxial $Co_2YZ$-based MTJs with a MgO tunnel barrier[3–6] and demonstrated high tunnel magnetoresistance (TMR) ratios of 179% at RT and 683% at 4.2 K for fully epitaxial $Co_2MnSi/MgO/Co_2MnSi$ MTJs.[6] These high TMR ratios at both a low temperature of 4.2 K and RT show that our approach of growing fully epitaxial MTJ layer structures with $Co_2YZ$ thin films and a MgO barrier is highly advantageous for fully utilizing high spin polarizations of potentially half-metallic $Co_2YZ$ electrodes.[6,15]

One Co-based Heusler alloy, in particular, $Co_2MnGe$ (CMG), features a theoretically predicted half-metallic nature[11–13] and a high Curie temperature of 905 K (Ref. 14). It also features a small lattice mismatch of −3.6% with MgO for a 45° in-plane rotation within the (001) plane. This small lattice mismatch, compared to, for example, that of −5.1% between $Co_2MnSi$ and MgO is preferable for realizing high-performance CMG-based MTJs with a single-crystalline MgO barrier. By comparison, previously reported $CMG/MgO/Co_{50}Fe_{50}$ MTJs showed lower TMR ratios of 83% at RT and 185% at 4.2 K (Ref. 5). Our purpose in the present study has been to clarify the key factors that determine the spin-dependent tunneling characteristics of $CMG/MgO/Co_{50}Fe_{50}$ MTJs. To do this, we investigated the effects that *in situ* annealing immediately after preparation of the MTJ trilayer, i.e., just after preparation of the interfaces in the MTJ trilayer had on the spin-dependent tunneling characteristics through a possible improvement of the electronic structure; in particular, that of the interfacial region.

The fabrication procedure was essentially the same as for the exchange-biased $CMG/MgO/Co_{50}Fe_{50}$ MTJs previously reported,[5] but we introduced *in situ* annealing just after deposition of the $Co_{50}Fe_{50}$ upper electrode. The fabricated MTJ layer structure was as follows: (from the substrate side) MgO buffer (10 nm)/CMG (50 nm)/MgO barrier (0.8–3.4 nm)/$Co_{50}Fe_{50}$ (3 nm)/Ru (0.8 nm)/$Co_{90}Fe_{10}$ (2 nm)/$Ir_{22}Mn_{78}$ (10 nm)/Ru cap (5 nm), grown on a MgO(001) substrate. The CMG lower electrode was deposited at RT using magnetron sputtering and subsequently annealed *in situ* at 500 °C for 15 min. The $Co_{50}Fe_{50}$ upper electrode was also deposited at RT. The MTJ trilayer was *in situ* annealed right after deposition of the $Co_{50}Fe_{50}$ upper electrode at various temperatures ($T_a$). TMR characteristics were investigated as a function of $T_a$ along with $dI/dV$ versus $V$ characteristics. We determined through inductively coupled plasma analysis that the CMG film composition used in this study was $Co_2Mn_{0.77}Ge_{0.42}$ with an accuracy of 2%–3% for each element. The fabricated junction size was $10\times10$ $\mu m^2$. We defined the TMR ratio as $(RA_{AP}-RA_P)/RA_P$, where $RA_P$ and $RA_{AP}$ are the respective resistance-area products for the parallel (P) and antiparallel (AP) magnetization configurations. We measured the differential conductance ($dI/dV$) versus $V$ characteristics of the fabricated MTJs using a conventional lock-in method with a typical modulation peak-to-peak voltage of 10 mV and a modulation frequency of 317 Hz. The bias voltage ($V$) was defined with respect to the CMG lower electrode, i.e., electrons tunnel from the CMG lower electrode to the $Co_{50}Fe_{50}$ upper electrode at a positive $V$.

Figure 1(a) shows typical MgO barrier thickness ($t_{MgO}$) dependence of $RA_P$ and TMR ratios at RT for a $t_{MgO}$ range from 1.2 to 3.0 nm for $CMG/MgO/Co_{50}Fe_{50}$ MTJs with $T_a$ of 475 °C fabricated on a $20\times20$ $mm^2$ MgO(001) substrate. $RA_P$ showed clear exponential dependence on $t_{MgO}$ for a relatively wide $t_{MgO}$ range from 1.8 to 3.0 nm (region-I), but deviated from the exponential dependence in the $t_{MgO}$ range below 1.8 nm (region-II). Note that, even though the values of $RA_P$ changed by about four orders of magnitude in the $t_{MgO}$ range from 1.8 to 3.0 nm, the TMR ratios were

a)Author to whom correspondence should be addressed. Electronic mail: yamamoto@nano.ist.hokudai.ac.jp.

 

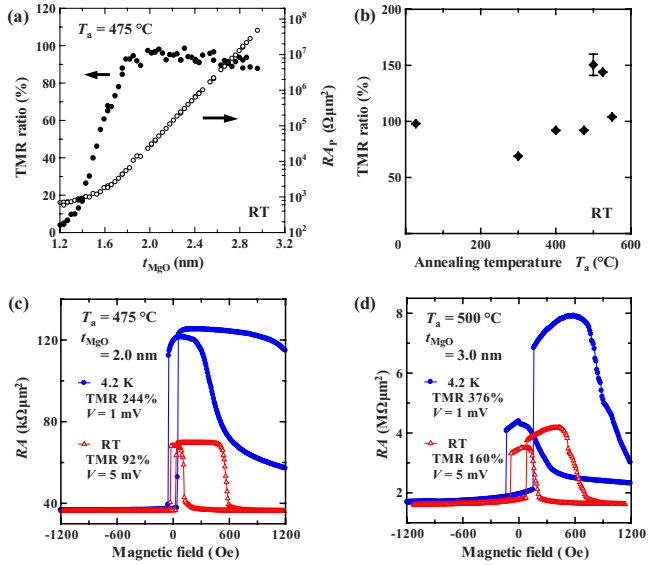


FIG. 1. (Color online) (a) Typical $t_{MgO}$ dependence of $RA_P$ and TMR ratios at RT for $Co_2MnGe/MgO/Co_{50}Fe_{50}$ MTJs with $T_a$ of 475 °C fabricated on a 20×20 mm² MgO(001) substrate, where $RA_P$ represents the resistance-area product $RA$ for the P configuration. (b) TMR ratios at RT as a function of $T_a$. The error bar for $T_a$ of 500 °C indicates the range of observed TMR ratios for MTJs fabricated on a 20×20 mm² MgO substrate. [(c) and (d)] Typical magnetoresistance curves at RT and 4.2 K for MTJs with (c) $T_a$ of 475 °C and $t_{MgO}$ of 2.0 nm and for those with (d) $T_a$ of 500 °C and $t_{MgO}$ of 3.0 nm. The bias voltage was 1 mV at 4.2 K and 5 mV at RT.

almost constant at 93% ± 2% (the absolute mean deviation) for this region, but decreased with decreasing $t_{MgO}$ below 1.8 nm. Taking into consideration this dependence of the TMR ratio on $t_{MgO}$, we will focus in the following on MTJs having $t_{MgO}$ values from region-I to discuss the influence of annealing on spin-dependent tunneling characteristics without $t_{MgO}$ being a factor.

Figures 1(c) and 1(d) show typical magnetoresistance curves at RT and 4.2 K for fabricated epitaxial $CMG/MgO/Co_{50}Fe_{50}$ MTJs with [Fig. 1(c)] $T_a$ of 475 °C and $t_{MgO}$ of 2.0 nm and for those with [Fig. 1(d)] $T_a$ of 500 °C and $t_{MgO}$ of 3.0 nm. The MTJs exhibited clear exchange-biased TMR characteristics. Note that the TMR ratio increased markedly with increasing $T_a$, rising from typical values of 92% at RT and 244% at 4.2 K for $T_a$ of 475 °C to 160% at RT and 376% at 4.2 K for $T_a$ of 500 °C. Furthermore, a plot of the TMR ratio at RT as a function of $T_a$ [Fig. 1(b)] shows clearly that the TMR ratio increased discontinuously and significantly with increasing $T_a$ from 475 to 500 °C. The TMR ratio decreased, however, as $T_a$ increased beyond 500 °C and the MTJ with $T_a$ of 550 °C showed a smaller TMR ratio of 104% at RT. We will mainly concern ourselves with the possible origin of the abrupt increase in the TMR ratio for MTJs with $T_a$ between 475 and 500 °C in the following.

To further investigate spin-dependent tunneling characteristics of $CMG/MgO/Co_{50}Fe_{50}$ MTJs, we measured $dI/dV$ (=$G$) versus $V$ characteristics for P and AP ($G_P$ and $G_{AP}$ spectra, respectively) at 4.2 K and RT. Figure 2 shows typical $G_P$ and $G_{AP}$ spectra at 4.2 K for $CMG/MgO/Co_{50}Fe_{50}$ MTJs with [Fig. 2(a)] $T_a$ of 475 °C and $t_{MgO}$ of 2.0 nm [the same MTJ as for Fig. 1(c)] and for those with [Fig. 2(b)] $T_a$ of 500 °C and $t_{MgO}$ of 2.9 nm which showed a TMR ratio of 322% at 4.2 K (144% at RT). The $G$ spectra of the MTJs with $T_a$ of 475 °C [Fig. 2(a)] exhibited distinct peak structures (1) at a characteristic voltage ($V_{C1+}$) of ~0.22 V (for $V>0$) for P, and (2) at $V_{C2-}$ of ~−0.38 V (for $V<0$) and $V_{C2+}$ of ~0.27 V (for $V>0$) for AP. These pronounced peak structures were also observed at RT with almost the same characteristic voltages of $V_{C1+}$, $V_{C2-}$, and $V_{C2+}$. Furthermore, these peak structures in $G_P$ and $G_{AP}$ spectra were commonly observed with almost the same characteristic voltages for MTJs fabricated with $T_a$ of 475 °C or less.

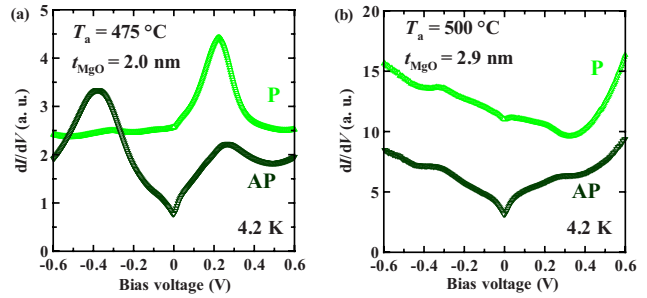


FIG. 2. (Color online) Typical $dI/dV$ vs $V$ characteristics for the parallel (P) and antiparallel (AP) configurations at 4.2 K for $Co_2MnGe/MgO/Co_{50}Fe_{50}$ MTJs with (a) $T_a$ of 475 °C and $t_{MgO}$ of 2.0 nm [the same MTJ as for Fig. 1(c)] and for those with (b) $T_a$ of 500 °C and $t_{MgO}$ of 2.9 nm showing a TMR ratio of 322% at 4.2 K (144% at RT). The bias voltage ($V$) was defined with respect to the $Co_2MnGe$ lower electrode.

Most importantly, these distinct peak structures observed for MTJs with $T_a$ of 475 °C or less completely disappeared for MTJs with $T_a$ of 500 °C at both 4.2 K [Fig. 2(b)] and RT (not shown). Furthermore, MTJs with $T_a$ higher than 500 °C (i.e., $T_a$ of 525 or 550 °C) showed $G_P$ and $G_{AP}$ spectra similar to those of the MTJ with $T_a$ of 500 °C. This revealed that the discontinuous and significant increase in the TMR ratio for MTJs with $T_a$ of 500 °C was associated with the distinct changes in the $G_P$ and $G_{AP}$ spectra that featured the disappearance of the peak structures.

We will now discuss possible origins of the distinct changes in the $G_P$ and $G_{AP}$ spectra. First, we can reasonably attribute the existence of the peak structures in the $G$ spectra for MTJs with $T_a$ of 475 °C or less to a possible existence of peak structures in the spin-dependent density of states of the electrodes or the interfacial regions of the electrodes facing a MgO barrier. Taking into consideration the abrupt disappearance of the peak structures in the $G$ spectra caused by the annealing at $T_a$ between 475 and 500 °C, it is improbable that the distinct changes in the $G$ spectra were due to a possible existence of peak structures in the density of states of the CMG lower electrode. This is because that the CMG lower electrode was already *in situ* annealed at 500 °C right after deposition of the CMG lower electrode. The $G_P$ and $G_{AP}$ spectra of the reference $Co_2Cr_{0.6}Fe_{0.4}Al/MgO/Co_{50}Fe_{50}$ MTJ, which was identically fabricated with $T_a$ of RT and showed a TMR ratio of 294% at 4.2 K (94% at RT), did not exhibit a peak structure, even though it was fabricated with $T_a$ of RT, like those observed for the $CMG/MgO/Co_{50}Fe_{50}$ MTJs with $T_a$ of 475 °C or less. This suggests that the possibility of peak structures in the density of states of the $Co_{50}Fe_{50}$ electrode or the interfacial region of the $Co_{50}Fe_{50}$ electrode facing a MgO barrier can be excluded. Thus, it is likely that peak structures exist in the spin-dependent density of states for the interfacial region of the CMG electrode facing a MgO barrier in MTJs with $T_a$ of 475 °C or less.

Figure 3 shows a model of the spin-dependent density of states for the interfacial region of the CMG lower electrode

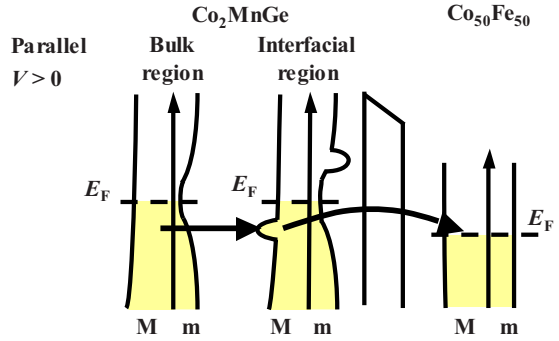


FIG. 3. (Color online) Schematic of a model of the spin-dependent density of states for the interfacial region of the $Co_2MnGe$ lower electrode in $Co_2MnGe/MgO/Co_{50}Fe_{50}$ MTJs with $T_a$ of 475 °C or less, including a schematic for a tunneling process for P around a positive $V$ of $V_{C1+} \sim 0.22$ V, at which the peak structure was observed in the $dI/dV$ vs $V$ characteristics. M and m refer to M-spin band and m-spin band, respectively.

facing a MgO barrier in MTJs with $T_a$ of 475 °C or less that we propose to explain the $G$ spectra of these MTJs. The model features the existence of a peak structure in the interfacial density of states for majority spins with a peak position about 0.25 eV [an intermediate value between $eV_{C1+}$ (0.22 eV) and $eV_{C2+}$ (0.27 eV)] below the Fermi level ($E_F$) and the existence of such a structure for minority spins with a peak position about 0.38 eV ($e|V_{C2-}|$) above $E_F$. We tentatively assumed that the peak position about 0.38 eV above $E_F$ for minority spins is above the bottom of the conduction band for minority spins because the energy difference of 0.38 eV from $E_F$ is too large for the conduction band edge from $E_F$ if we compare it to one-half the theoretically predicted value of a half-metal gap of 0.21–0.54 eV for CMG.[11,12] For the bulk region of the CMG lower electrode, we tentatively assumed the existence of residual states in the possible minority-spin (m-spin) band gap, although this is not critical for the model of tunneling process that we will describe.

We will now examine possible tunneling processes for $V>0$ responsible for the peak structures in the $G_P$ and $G_{AP}$ spectra. A possible tunneling process for P around a positive $V$ of $V_{C1+} \sim 0.22$ V, at which the peak structure was observed in the $G_P$ spectrum is illustrated in Fig. 3, where electrons in the majority-spin (M-spin) band of the bulk region of the CMG lower electrode tunnel to the M-spin band of the $Co_{50}Fe_{50}$ upper electrode through the M-spin interface states in the interfacial region of the CMG lower electrode facing a MgO barrier. For $V$ around 0.22 V, the $G_P$ value is enhanced because of the existence of the peak around 0.25 eV below $E_F$ in the M-spin interfacial density of states, resulting in a peak structure in the $G_P$ spectrum around $V$ of 0.22 V ($V_{C1+}$). The peak structure observed in the $G_{AP}$ spectrum around 0.27 V ($V_{C2+}$) is similarly explained. The tunneling process for this case is essentially the same as that for the former case (for P and $V>0$), except that electrons tunnel to the m-spin band of the $Co_{50}Fe_{50}$ upper electrode.

For $V$ around −0.38 V ($V_{C2-}$), the $G_{AP}$ value is also enhanced because of the existence of the peak structure in the m-spin interfacial density of states with a peak position about 0.38 eV above $E_F$.

According to our explanation of the peak structures in the $G$ spectra based on the existence of peak structures in the interfacial density of states, it is most reasonable to attribute the discontinuous disappearance of the peak structures in the $G$ spectra caused by *in situ* annealing at $T_a$ between 475 and 500 °C to a possibly substantial change in the interface states at the CMG electrode-MgO barrier interface. We tentatively attribute the existence of the peak structures in the interfacial density of states for MTJs with $T_a$ of 475 °C or less to unstable interface bonding. We suppose that these peak structures in the interfacial density of states disappeared with the change in the interface bonding to thermodynamically stable interface bonding caused by *in situ* annealing at $T_a$ between 475 and 500 °C. The marked increase in the TMR ratio can consistently be attributed to the rearrangement of the spin-dependent interfacial density of states, resulting in increased spin polarization in the interfacial region of the CMG electrode facing a MgO barrier.

In summary, the TMR ratio of fully epitaxial $CMG/MgO/Co_{50}Fe_{50}$ MTJs increased discontinuously and significantly from 92% at RT (244% at 4.2 K) to 160% at RT (376% at 4.2 K) when $T_a$ was increased from 475 to 500 °C. In addition, the $G_P$ and $G_{AP}$ spectra changed discontinuously and markedly when $T_a$ was increased from 475 °C or less to 500 °C or higher, and we ascribed this to a possible change in the interfacial bonding at the CMG electrode-MgO barrier interface from thermodynamically unstable bonding for MTJs with $T_a$ of 475 °C or less to stable bonding for MTJs with $T_a$ of 500 °C or higher. The significant increase in the TMR ratio with increasing $T_a$ from 475 to 500 °C was consistently explained in terms of increased interfacial spin polarization at $E_F$ associated with the change of the spin-dependent interfacial density of states.

This work was partly supported by a Grant-in-Aid for Scientific Research (A) (Grant No. 20246054) and a Grant-in-Aid for Scientific Research on Priority Area "Creation and control of spin current" (Grant No. 19048001) from the MEXT, Japan.

[1] N. Tezuka, N. Ikeda, S. Sugimoto, and K. Inomata, Jpn. J. Appl. Phys., Part 2 **46**, L454 (2007).
[2] Y. Sakuraba, M. Hattori, M. Oogane, Y. Ando, H. Kato, A. Sakuma, T. Miyazaki, and H. Kubota, Appl. Phys. Lett. **88**, 192508 (2006).
[3] T. Ishikawa, T. Marukame, H. Kijima, K.-i. Matsuda, T. Uemura, M. Arita, and M. Yamamoto, Appl. Phys. Lett. **89**, 192505 (2006).
[4] T. Marukame, T. Ishikawa, S. Hakamata, K.-i. Matsuda, T. Uemura, and M. Yamamoto, Appl. Phys. Lett. **90**, 012508 (2007).
[5] S. Hakamata, T. Ishikawa, T. Marukame, K.-I. Matsuda, T. Uemura, M. Arita, and M. Yamamoto, J. Appl. Phys. **101**, 09J513 (2007).
[6] T. Ishikawa, S. Hakamata, K.-i. Matsuda, T. Uemura, and M. Yamamoto, J. Appl. Phys. **103**, 07A919 (2008).
[7] K. Yakushiji, K. Saito, S. Mitani, K. Takanashi, Y. K. Takahashi, and K. Hono, Appl. Phys. Lett. **88**, 222504 (2006).
[8] T. Furubayashi, K. Kodama, H. Sukegawa, Y. K. Takahashi, K. Inomata, and K. Hono, Appl. Phys. Lett. **93**, 122507 (2008).
[9] X. Y. Dong, C. Adelmann, J. Q. Xie, C. J. Palmstrøm, X. Lou, J. Strand, P. A. Crowell, J.-P. Barnes, and A. K. Petford-Long, Appl. Phys. Lett. **86**, 102107 (2005).
[10] M. C. Hickey, C. D. Damsgaard, I. Farrer, S. N. Holmes, A. Husmann, J. B. Hansen, C. S. Jacobsen, D. A. Ritchie, R. F. Lee, G. A. C. Jones, and M. Pepper, Appl. Phys. Lett. **86**, 252106 (2005).
[11] S. Ishida, S. Fujii, S. Kashiwagi, and S. Asano, J. Phys. Soc. Jpn. **64**, 2152 (1995).
[12] S. Picozzi, A. Continenza, and A. J. Freeman, Phys. Rev. B **66**, 094421 (2002).
[13] I. Galanakis, P. H. Dederichs, and N. Papanikolaou, Phys. Rev. B **66**, 174429 (2002).
[14] P. J. Webster, J. Phys. Chem. Solids **32**, 1221 (1971).
[15] T. Saito, T. Katayama, T. Ishikawa, M. Yamamoto, D. Asakura, and T. Koide, Appl. Phys. Lett. **91**, 262502 (2007).